DOI: 10.13009/EUCASS2017-445

DOI: 445

Conceptual Design of Distributed Propeller Aircraft: Linear Aerodynamic Model Verification of Propeller-Wing Interaction

Baizura Bohari[†‡] *[*]Murat Bronz [†]Emmanuel Benard [‡]and Quentin Borlon [§]
[†]*ENAC, UAV Laboratory F-31055*
7 Avenue Edouard Belin, 31000 Toulouse, France
[‡]*ISAE-SUPAERO,*
Dept. of Aeronautic and Space Vehicles Design (DCAS)
10 Edouard Belin, 31055 Toulouse cedex 4, France
baizura.binti-bohari@isae-supaero.fr · murat.bronz@enac.fr
emmanuel.benard@isae.fr · quentin.borlon@student.isae-supaero.fr
[†]baizura.binti-bohari@isae-supaero.fr

Abstract

This paper opens an exciting new opportunity of new aircraft concepts specifically targeting to have higher aerodynamic efficiency than conventional designs through the synergistic interaction between the propeller and the wing. Previous literature on propeller and wing performance analysis methods provide a platform on theory description behind the aerodynamic modeling approach selected. The research effort began with attempts to verify previous NASA wind-tunnel tests (TN D-4448) on a medium and short wing span propeller-driven, short take off and landing (STOL) transport aircraft. One prediction is employed on isolated performance of the wing without the propellers and another is to capture one-way coupling, specifically the effect of the propeller slipstream on the wing. For the first decoupled analysis configuration, the vortex lattice model (VLM) technical tools comparison was made with the Athena Vortex Lattice (AVL) and VSPAERO. Next, the propeller and the wing interaction is predicted using three different coupling methods. The first stage of the work is based on VSPAERO solver which combined the actuator disk theory with VLM. The second approach is to compare with the in house code of blade element and lifting line theory (LLT) coupling. Thirdly, to couple the same BET model with VLM to capture the aerodynamics performance and the influence of the propeller on the wing with the aim to determine the lift and induced drag of the configuration. Perhaps the most compelling aspect offered by the technical tools selected is being economic; low computational cost and time. The numerical computation results of the model presented a good correlation with the experimental data. The aerodynamic model developed will be a strong base for more complex analysis and even greater efficiency improvements for a conceptual design studies of future distributed propeller aircraft .

1. Introduction

In recent years the research milestones of distributed propeller operated engine along the wing of the aircraft has evolved tremendously, both experimentally and numerically. To begin with, the effectiveness of distributing small gas-turbines along an aircraft span was examined to increase propulsive and airframe structural efficiency.[2] However, the thermal efficiency is reported to be poor for smaller engines due to scaling effects, so the electrical distribution of power to motorised fans may provide a more efficient solution to enable distributed propulsion. Overall system weight reduces with increasing number of motorised fans, in contrast with predicted increasing weight for small gas turbines,

[*]Doctoral Student at ENAC and ISAE-Supaero sponsored by the Department of Mechanical Engineering, National Defense University of Malaysia, Kem Sg. Besi, 57000 Kuala Lumpur, Malaysia
[†]Assistant Professor-Applied Aerodynamics, ENAC, UAV Laboratory F-31055
[‡]Associate Professor-Aircraft Design, Dept. of Aeronautic and Space Vehicles Design (DCAS)
[§]Double Degree Student, Dept. of Aeronautic and Space Vehicles Design (DCAS)

DOI: 10.13009/EUCASS2017-445

which get heavier due to their auxiliary systems and non-scalable parts (which will still be present with electric power transmission but to a reduced extent).[2] The success of the concept however, hinges on the superconducting machines power density capabilities, which currently are below the required level and therefore the concept is targeted for a 2035 timeframe. The aircraft may be specifically designed to efficiently carry the extra electrical system associated mass, therefore stressing the highly integrated nature of the distributed propulsion technology.

Moving forward, NASA has extended the LEAPTech demonstrator analysis by comparing the numerical analysis[21] with the experimental results.[22] Previously, they have gain a rise in maximum lift coefficient, drag reduction through a number of electric motor driving individual tractor propellers spaced along the wingspan. Apart from that, they figure that depending on flight conditions this configuration could provide significant efficiency gains in higher-speed aircraft, even greater advantage for high wing loading as well as larger aircraft. The simulation part of the project is aligned with the geometry modelling and research interest here. The work is widely spread around various higher-order fidelity aerodynamic computational tools, namely, STAR-CCM+ and FUN3D RANS code as well as low-order fidelity, the VSPAERO[17] vortex lattice code. Both, numerically and experimentally predicted performance were validated. In much recent achievement, NASA introduced more advance propellers[4,20] and the resulting SCEPTOR (Scaleable Convergent Electric Propulsion Technology Operation Research) concept aims at demonstrating large impacts on the performance of the high-lift system, lower weight, lower volume, thus, less vibration as compared to conventional internal combustion or gas turbine aircraft.

As the newly proposed concept laid a promising research milestone, NASA introduced more advance propellers which not only act as a thrust source but also has similar function as a high-lift device.[4,20] The SCEPTOR (Scaleable Convergent Electric Propulsion Technology Operation Research) demonstrator likely to have large impacts on the performance of the high-lift system, lower weight, lower volume, thus, less vibration as compared to conventional internal combustion or gas turbine aircraft. The aerodynamic sizing is based on a mix of low fidelity methods, validated by high fidelity simulations. Initial parametric blade shape profile (chord and twist distribution) and airfoil shape were formulated with MATLAB® and then fed into Xfoil[9] to be analyze.[5] The post-processing results with XROTOR[11] particularly resume that the airfoil shape had a significant impact on the chord distribution which indeed challenge the existing propeller design practise. Ultimately, these contributions may lead to advantageous aeropropulsive coupling evenly distrubuted over the airframe.

A paper presented by Ferraro et al.[12] proposed a method to account for propeller slipstream effects on a finite wing for early design stage. In this study, the test case models, namely a four-propeller aircraft and a CROR propeller aircraft, were developed and tested against the aerodynamic model consist of a Truckenbrodt 3D lifting surface method coupled with a 2D numerical solver, MSES.[8] The airfoil numerical solver method used to consider viscosity and camber effects and a Blade Element Theory (BET), combined with momentum conservation equations for the formulation of the propeller aerodynamics. The findings were validated against RANS CFD and wind tunnel experimental data where they find a considerably good consistency of performance across different geometries and flow conditions. A very economical computational cost as compared to the use of more sophisticated flow solver is a compliment to the approach presented which might be appropriate for further extensive studies on Multi-Disciplinary Optimisation (MDO). In extension to that, a rapid approach model by Agostinelli et al. captured the effects of propeller slipstream aerodynamic using RANS-Actuator Disk model.[1] The RANS-Actuator Disk computation combined the Blade Element Momentum Theory (BEMT) for the propeller sipstream modelling with the RANS database of the wing loading variation without the propeller effects with respect to number of flight incidences. The simulation was then validated and went through the optimisation process in a quest for the optimum position of the propeller. As a results, the rapid approach was found in close agreement with the high fidelity method in all cases except for its failure to capture the peaks in lift coefficient.

In general, the framework in the pre-conceptual design concepts includes the principal dimensions, aerodynamics parameters, weight, propulsion system characteristics, and flight performance. In the initial stage, the most common design process utilizes semi-empirical methods followed by the detailed shape defining the aircraft configurations in Computer-Aided Design (CAD) environment. In combination with the preliminary results, numerical flow simulations using computational fluid dynamics (CFD) are conducted accordingly based on the CAD geometry of the aircraft model to classify potential parameters involved and constraints affect the overall propulsive efficiency. The results of the flow simulation can be further elaborate in verifying and calibrating the methods and assumptions made initially in the overall aircraft design and sizing models.The aerodynamic calculations for a given geometry from the CAD module are divided into three groups:

Tier I: Linear aerodynamics methods, mainly Vortex Lattice Method (VLM) that in this case cover low speeds and low angles of attack of the aircraft i.e. VSPAERO and AVL software.

DOI: 10.13009/EUCASS2017-445

Tier II: For high-speed aerodynamics problem will be solve with Panel Method i.e. PANAIR software.

Tier III: High-fidelity analysis is to extract accurate solutions from extreme flight conditions. However, more effort have to be put in this RANS (Reynolds-averaged Navier-Stokes method) in terms of mesh creation and computational time cost i.e. CFD software.

Figure 1 shows the design process workflow design process of our intial multi-disciplinary design studies on linking the propulsion, mass, aerodynamics and performance analysis block using xDSM standard.[16] The different modules and their interactions shown are related to a specific aspect of conceptual design. For every rectangular block represents an anlysis where grey block means the input and output. The two different lines, grey and black line are the data connection and workflow line respectively. The aerodynamics performance analysis was based on mass flow through the engine where the module models the thrust required which closely linked to the total aircraft weight including the engine of the aircraft. The aerodynamic analysis will also form the basis of a multidisciplinary design, analysis, and optimization (MDAO) framework that will be used to perform conceptual design studies of the distributed propeller configuration. For this reason, parametric analysis of the baseline airframe selected will help to manage the sensitivity integration between the aerodynamic and propulsion system in the earlier stage of conceptual design. The synergy through a full suite of multidisciplinary disciplines, which vary most significantly from traditional design, could provide beneficial effects such as aerodynamic/propulsion efficiency improvement.

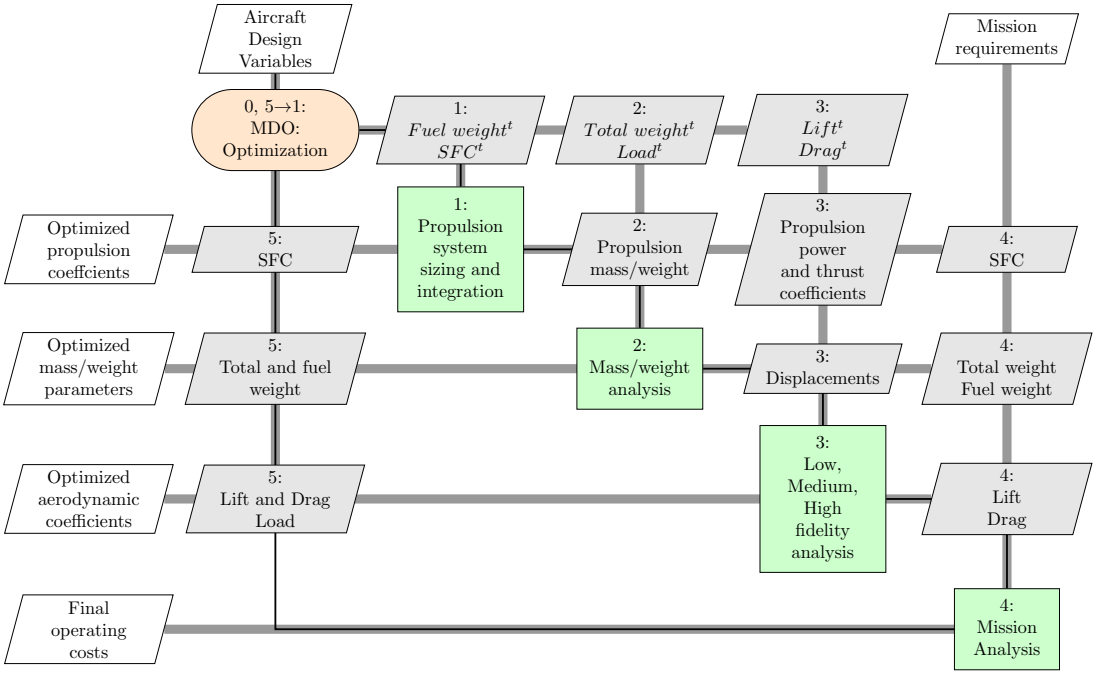

Figure 1: Multidisciplinary design optimization (MDO) workflow process

This paper presents alternative methods for a quick and accurate assessment, aiming to improve the prediction of the aerodynamics behaviour in the pre-design stages. The proposed methods in this work models the aerodynamic performances with VLM as well as coupling algorithm of Prandtl lifting line and blade element theory. The evaluation of the quantitative flow analysis behind the propeller-wing model were focused on the ability of the wake flowfield to produce accurate information about the lift and the drag components when the propeller slipstream interacts with the wing. Additionally, to demonstrates the value of the measurement techniques on the wing aerodynamic performance from the deformed slipstream and vortex wake downstream of the wing as it is important for future optimization of distributed propeller-wing configurations. This paper is organized in four main sections. Section 2 review on the theoretical background and methodological contributions of this topic. The implementation process of the methods applied, geometry representation and test case set up were briefly discussed in section 3 and 4.The results of the numerical computation and comparison with the experimental data were highlighted in section 5. Finally, in the last section concludes the main achievements of this research work and potential area of research are suggested for future work.

DOI: 10.13009/EUCASS2017-445

2. Modeling Framework of Linear Propeller-wing Method

In a quest for sufficiently simple and practical analysis methods, at the same time lies the difficulty where these methods should be sophisticated enough to capture distinct changes in the local geometry. It is a complex task as it involves radical changes conceptually and technically. In the process of determining a set of more appropriate aerodynamic models, tests with different configurations must be conducted during the preliminary and conceptual design phase. The main focus of this section is to describe the principles and fundamentals of aerodynamic models in propeller-wing interaction effects for a typical propeller-driven aircraft. With the establishment of the basic characteristics, the theoretical foundation and the interaction effects of a standard propeller-wing configuration, the step towards numerical techniques in integrating a propeller, nacelle and wing is taken.

There are a couple of distinct researches related with slightly different approaches computationally and experimentally available. Witkowski et al. conducted both wind tunnel test and computational investigation to addresses the aerodynamic interaction between propellers and wing.[23] From the wind tunnel test, they have discovered other than drag reduction and lift increament, the maximum benefit of propeller and untapered, unswept semi-span wing model combination is at the lower power condition. Computationally, they have concluded an accuracy range of (10-30% for $\triangle C_D$) for semi-empirical formulation and (6-12% for $\triangle C_D$) for VLM. Moens and Gardarein approached the topic with extra computing cost using Euler and 3D Navier-Stokes computation.[18] The scope of work covered 3D rectangular wing mounted with a 3-element airfoil with double-slotted flap system at take-off and cruise conditions. Despite a higher computing cost, both computation model have been accurately predicted using actuator disk model for the propeller part.

In the direction of lower computational cost, Hunsaker and Deryl modeled BET combined with momentum conservation equations for the propeller, then integrated with a lifting-line approach for the wing part.[13] The propeller-wing combine method tend to over-predicted the magnitude of the lift perturbations as a result of the slipstream effect from the propeller. The work has not taken into account a high-lift configuration attached to the wing. Very recently, Jardin et al. have revisited the Froude's theory and extends the free propellers analysis to the shrouded rotor in the context of micro-air vehicles applications.[14] In particular, they have formulated analytical model of the total, rotor, shroud, upstream shroud, and downstream shroud thrusts as well as induced power for each component system. The sensitivity of the model to viscous effects is highlighted and the results provide insight to the aerodynamic of shrouded rotors globally. Recently published work has extended the classical model of steady actuator disk to unsteady flows.[7] The approach allows variations of shed vorticity to account for the flow conditions at the disk instead of constant vorticity in steady flow. The results of the new derived model show good agreement with two sets of experimental data, from field as well as wind tunnel measurements.

Like a wing, a propeller profile is an airfoil geometry that will generate an aerodynamic force very much the same way. In the field of general aviation, the propeller is rotated by the engine and thus creates thrust to propel the aircraft forward. There are three theories primarily used in the design of propellers, namely 1) momentum theory, 2) blade element theory and 3) vortex theory. Until recently the first two theories were more often employed in practical calculation. This is primarily due to the mathematical complexity of the vortex theory. Most of today's propellers were designed depended on a principle of independence of blade elements. The existing propeller design is essential to be adapted to the designer's requirements. During the early design phase, one of the inputs is the thrust curve of the power plant available thrust against flight velocity. It is of interest to evaluate and compare aircraft performance and discover configuration characteristics via the iterative optimization procedure, which requires rapid analysis of prospective engines and propellers. The preliminary design work of an aircraft has been divided into different phases due to the increase of the numerical power of machine. Different approaches presented here show a strongly coupled algorithm with the gain in accuracy at reasonably low computational costs. The effect of the propellers in front of the leading edge of the wing analysis first take into account the VLM coupled with actuator disk theory which was implemented using VSPAERO. In parallel, the second scope of work consists of both using BET coupled with lifting line theory (LLT) and the other is VLM to resolve the effect of the propeller slipstream on the wing performances.

The LLT and VLM methodologies are well-known and widely accepted for conceptual design steps. They provide reliable results and lot of work were already done to generalised the method up to the viscous case. These approaches to modeling the propeller flowfield stays well within LLT limitations i.e., high aspect ratio, low mach number (compressibility effects may be neglected at first order) and small sweep. With a rapid development of computer capacity and efficiency, the application of the VLM was challenged with more complex configuration design namely multi-planes, nonplanar wings, wing tip and interference. To incorporate the propeller slipstream effect into the VLM algorithm can

DOI: 10.13009/EUCASS2017-445

be unique utilisations of the VLM, of lattice analytical advancements, and the power and nature of this new discipline. The interaction between the propeller and other aerodynamic surfaces of the aircraft will have the greatest impact on the overall aerodynamic performance of the aircraft.

2.1 Actuator Disk Theory and Vortex Lattice Method Coupling (VSPAERO)

In presenting the effects of the propeller induced flow on the aerodynamic performance of the wings correspond to the tractor configuration propeller fairing set up, the VSPAERO perform rapid aero-propulsive analysis. VSPAERO is a well recognized computational mean adopting vortex lattice solver developed with a simple actuator disk model to represent the flow over a section of panels behind a propeller. The flow over a section of panels behind a propeller can be analyzed by implementing actuator disks into the solver, which modifies the local freestream to account for increased speed and vorticity induced by the propeller. For a freestream/glide condition analysis, the actuator disks may be left inactive (empty). In general, a propeller-theoretical model developed from the fundamental momentum principles/actuator disk theory may lead to a useful insight of propeller inflow and slipstream characteristics.

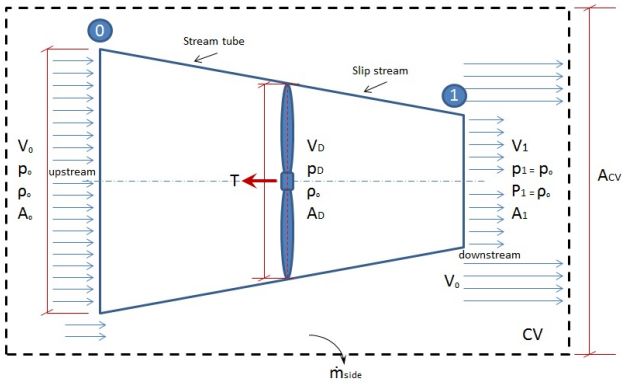

Figure 2: Definition sketch of one dimensional actuator disk model in uniform flow.

As an aid to the discussions, from general momentum theory shown in Figure 2, dimensionless analysis leads to a number of useful coefficients with the C_P as power non dimensionalised by available power through disk area, A and freestream velocity, V in which similarly applied in defining the C_T for thrust,

$$C_P = \frac{P}{\frac{1}{2}\rho V_0^3 A_1} \tag{1}$$

$$C_T = \frac{T}{\frac{1}{2}\rho V_0^2 A_1} \tag{2}$$

Alternatively, introduced below various dimensionless parameters used in propeller performance work, thrust coefficient, C_T, power coefficient, C_P and advance ratio, J, respectively

$$C_P = \frac{P}{\rho n^3 d^5} \tag{3}$$

$$C_T = \frac{T}{\rho n^2 d^4} \tag{4}$$

$$J = \frac{V_0}{nd} \tag{5}$$

P defines the power input to the propeller ($N\frac{m}{s}$ or $ft\frac{lbf}{s}$), n is the rotational speed of the propeller ($\frac{rev}{s}$), d is the diameter of the propeller in m. The propeller efficiency, η can also be measured in terms of C_T, C_P and J as follows:

$$\eta = \frac{C_T}{C_P} J \tag{6}$$

In some cases, a torque coefficient, C_Q can be a replacement to the C_P with propeller shaft torque, Q through disk area and relationship of $P = 2\pi nQ$

$$C_Q = \frac{Q}{\rho n^2 d^5} \tag{7}$$

DOI: 10.13009/EUCASS2017-445

This led to

$$C_P = 2\pi C_Q \tag{8}$$

Alternatively, in a similar manner the propeller efficiency can also be expressed with,

$$\eta = \frac{C_T}{2\pi C_Q} J \tag{9}$$

Despite the complexity of the real flow, this simplified approach allows the thrust and torque to be calculated provided that some of the appropriate values are made available. From a numerical standpoint, actuator disk model is often the option to extensively study the downstream wakes and their effects despite its limitation to capture the boundary layer development.

2.2 Blade Element and Lifting Line Theory Coupling (BLLT)

This section introduced a rather straight forward low order linearized technique and tool, but at the same time relatively precise dedicated for the propeller-wing analysis. However, the linearity has become one of a major drawback of this classical technique as well where it does not predict stall. The implementation of Prandtl lifting line theory (LLT) and the blade element theory (BET) coupling in Matlab code generated a simplified propeller-wing geometry with the inputs of the wing geometries, propeller parameters and the definition of the case anlysis. With those data, the configuration is simulated and the flow field has to be converged with the aerodynamical coeffcients and the lift distribution along the span are plotted by solving several aerodynamic equations simultaneously. The essential of the lifting line tool computes three aerodynamic force coefficients of a given configuration, namely, the lift force, side force and induced drag. The integration of the circulation over the wing spanwise results in the lift and side force computation. For the determination of the induced drag force the integration of the circulation over the entire wing projected into the Trefftz-plane, far behind the wing. The circulation law in the form of three-dimensional:

$$\Gamma(y) = \frac{C_{l\alpha}(y)}{2} V_e(y) l(y) (\alpha_0(y) - \alpha_e(y)) \tag{10}$$

where $C_{l\alpha}(y)$ is the slope of the airfoil in the section y, V_e is the effective speed of the flow, which hit the leading edge, $l(y)$ is the length of the chord in the section y, α_0 is the zero lift angle of attack of the airfoil in y section and α_e is the effective angle of attack of the airfoil. The effective velocity is define as the sum of the sliding surface velocity and the freeflow velocity , neglecting the contribution of the induced speed of the propellers $V_{i\theta}$ and the induced velocity due to the circulation v_i.

$$V_e = [(V_\infty + V_{ix})^2 + (V_{i\theta} + v_i)^2]^{1/2} \approx V_\infty + V_{ix} \tag{11}$$

The effective angle of attack of the flow is define as the sum of the contributions of all the induced velocities and the free flow speed:

$$\alpha_e = \alpha + \frac{V_{i\theta}}{V_\infty + V_{ix}} + \frac{v_i}{V_\infty + V_{ix}} \tag{12}$$

This tool computes two dimensional wing geometries and the polar computation of the airfoils at specified Reynolds numbers are performed using the open-source XFOIL tool. Based on the reference airfoil geometry input the lift slope and zero-lift angle of attack can be calculate directly. The BET main task is to capture the results of induced velocities generated in the propeller's slipstream with the input of the required thrust, diameter, rotational speed of the propeller and the flight condition i.e., velocity and density of the flow. Here, how the induced velocity V_{ix} can be deduce from the thrust developed by the actuator disk, T with surface, S and freestream velocity, V_∞ input:

$$V_{ix} = \frac{V_\infty}{2} \left(\sqrt{1 + \frac{2T}{\rho S V_\infty^2}} - 1 \right) \tag{13}$$

The next part is to connect the axial induced velocities and tangential through a balance rothalpy directly downstream of the rotor plane:

$$V_{i\theta} = a'.2\Omega r \tag{14}$$

DOI: 10.13009/EUCASS2017-445

where a' is the induction factor determine with:

$$a' = \frac{1}{2}\left[1 - \sqrt{1 - 4a(1+a)\left(\frac{V_\infty}{\Omega r}\right)^2}\right] \tag{15}$$

and the factor a:

$$a = \frac{V_{ix}}{V_\infty} \tag{16}$$

where Ω is the rotational speed and r is the relative distance to the rotor shaft.

2.3 Blade Element and Vortex Lattice Method Coupling (BVLM)

The low computing cost makes VLM a practical tool for solving complex non-linear aerodynamic problems. It implies extremely simple concept, based on solutions to Laplace's Equation to assist aerodynamicist in estimating aircraft aerodynamics. VLM are subjected to some basic theoretical restriction namely, dedicated for incompressible, inviscid and irrotational flow field. The boundary conditions are applied on a mean surface, not the actual surface. Thin lifting surfaces combinations where the influences of thickness on aerodynamic forces are neglected. The classical description of the vortex lattice method is taking into account the basic horseshoe vortex model. The VLM is a generalisation of the lifting line theory for wing with reasonable sweep and dihedral.

A deeper understanding of the method, will lead to lift and induced drag computation with the lifting surfaces such as aircraft wings, fins and canards modelled as an infinitely thin sheet of discrete vortices. The lifting areas were divided into a lattice of quadrilateral panels and each panel has horseshoe vortex. Corresponding to the Prandtl lifting line theory, the finite line of the horseshoe vortex is located on the 1/4 chord element line and the control point at 3/4 chord point of each panel positioned at the midpoint in the spanwise direction. This 1/4-3/4 concept has a fundamental role in predicting the section lift and moment for constant angle of attack of thin wing theory. The circulation, Γ remains constant along the vortex line. The classical description of the vortex lattice method is taking into account the basic horseshoe vortex model. More details on the general VLM method have been addressed by several authors[6,3] More informations can be found in reference[15] written by Katz and Plotkin on the VLM method.

The method used here is to model the propeller-wing interaction using the same BET model in the BLLT code coupled with the VLM method. The method consists in dividing the wing into panels that lie on the mean camber "sheet" of the wing. Generally, the wing is divided along both the span and the chord. A panel is now also divided into sub-panels thanks to the chordwise distribution. The thinner the distribution, the more realistic to the actual geometry the linear prediction step will be and the linear approximation will be accurate, in the linear domain of the polar. If the wing is sufficiently discretized, the meshed wing in the VLM will have for any spanwise segment the same zero-lift angle and lift curve slope than the one in the 2D polar file. To do this, a highly accurate geometric description of the wing is necessary. Naturally, all the stall effect are not predicted because the VLM is a linear theory, each spanwise panel (not sub-panel) is characterised by two things namely, the zero-lift angle and the lift curve slope. It is known since a long time that the lift curve slope of a sub-panel depends on the distance between the bound-vortex and the collocation point . The point where the tangency condition is satisfied. Because we know for each panel the lift curve slope, we can adjust the distance between the bound-vortex, at quarter-chord, and the collocation point (h):

$$\frac{h}{c} = \frac{c_{l,\alpha}}{4\pi}.$$

What we have here are both parameters fixed and no chordwise discretisation of the panel was necessary to keep the computational cost at the lowest for a given number of panels along the span. Each spanwise panel may be modelled as a flat rectangular panel, with its corner on the leading and treading edge at the station y_i. This model takes into account light sweep, dihedral angles and the twist angle through the geometric description of the wing.
After the design step, the wing is initially discretized in n spanwise panels following a cosine distribution. The panel i lies between y_i and y_{i+1} where :

$$y_i = \frac{b}{2} * cos\left(\frac{(i-1)\times\pi}{n}\right), i \in \{1, ..., n\}.$$

Where n is let free to the user. For any panel, a two-dimensional (2D) polar data is affected. This polar data is based on the corresponding airfoil and flow properties of the corrsponding wing segment. The next step is the construction of an

DOI: 10.13009/EUCASS2017-445

influence coefficients matrix $\mathcal{A}$ thanks to a VLM code. This matrix is only dependent on the lifting surfaces geometry and the lift curve slope of the 2D data. The right-hand-side of the VLM method takes into account the zero-lift angle of the panels and the influence of the propellers through a blade element theory. The solution of the VLM method provides a linear prediction. Once all the above preparation steps are done, the real computation begins where the lift and drag curves will be computed to predict the propeller effects on the wing.

3. Tools Review and Test Configuration

The implementation of propeller effects in the VLM and LLT will be discussed. Alternative technical tools that were considered that involve a VLM formulation and models of the wing and propeller analysis are AVL[10] and VSPAERO.[17] As a part of this aerodynamic modeling, the performance analysis of the wing and propellers must be predicted to determine the lift and induced drag of the configuration base on a four propeller wing airframe selection from NASA TN D-4448 Report. The general specifications of the test model is presented in Table 1 for two different wing span. Thrust coefficients were also varies to monitor the effects on lift augmentations. The direction of propeller rotations were also observed with the variation of angle of attacks and spanwise variation of propeller thrust.

The model was tested in Langley 300 MPH 7- by 10 foot tunnel at various free-stream dynamic pressures and propeller thrusts. The wing-propeller combination model test, wing and propeller individual test were conducted up to 90 deg angle of attack. Method of analyzing and interpreting the relevant interaction effects are summarized with the short and medium wing span undergone variation of angle of attack with a constant wind tunnel dynamic pressure, propeller speed and propeller blade angle for each run. To have a constant and equal propeller thrust with the spanwise variation, the inboard propeller blade angle was set up at 16 degree while the set up of the outboard propeller is at 0 degree. Shown in Figure 3a is an OpenVSP model geometry constructed based on the planform shape given in table 1, airfoil coordinates, fuselage cross-section shape, and nacelle without imposing the actuator disk. As in Figure 3b has four propellers with a diameter of 2.84 m attached to the nacelle.

Table 1: Model geometry.[19]

Dimension	**Short wing span**	**Medium wing span**
Span, m	13.21	14.61
Area, m^2	30.6	32.8
Mean aerodynamic chord, m	2.38	2.32
Aspect ratio	5.71	6.52
Taper ratio	0.554	0.507
NACA airfoil section	632-415	632-415
Sweep of leading edge, deg	2.88	2.88
Root chord, m	2.98	2.98
Tip chord, m	1.65	1.51

As for the second approach of the methodology, the code has been implemented in MATLAB® R2014b taken into account the thrust and the diameter of the propeller. With the inputs the flow parameters such as density and velocity, the velocity induced by the propeller can be obtain. After computing these velocities, the next step is the resolution of the equation system of the Prandtl lifting line. There are three important parts in BLLT GUI interface as featured in 4 namely, the definition of the flow, the definition of the geometry and the characteristics of the propellers. As a results of the wing and propellers representation the model compute the induced velocity produced by the propellers on the wing. The numerical trade off of the code for being low-cost and fast is that it is limited to wings with propellers, and does not concern fuselages, empenages or other part of the plane.

An improvement of the second approach lead the authors to the third numerical model. Figure 5 shows the BVLM GUI of the developed tool featured on how the wing has to be designed from the root to the tip and each wing segment is characterised by its own characteristics (taper ratio, increment of twist, sweep, dihedral, airfoil, polar file (useful in case of same airfoil but change of aerodynamical behaviour), allowing discontinuities from one panel to the next in term of those characteristics. The evolution is assumed to be linear along a segment. A polar file is required and the file must be based on the actual geometry of the considered segment. Moreover, to enhance the accuracy of the results, this file must be based on the local Reynolds number, based on the mean aerodynamic chord of the wing segment and effective Mach number. For any of these airfoil data, the zero lift angle and the lift curve slope in the linear domain is computed. The 2D aerodynamics characteristics of the spanwise section will be obtained using MSES, Xfoil or directly

DOI: 10.13009/EUCASS2017-445

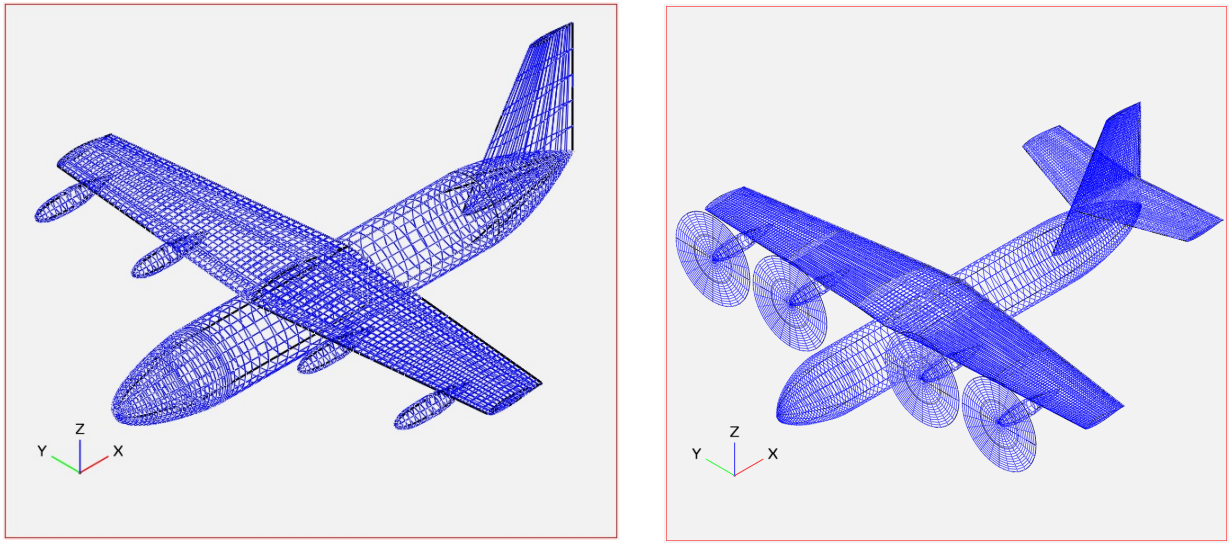

(a) Propellers off model

(b) Propellers on model

Figure 3: Open VSP Model geometry representation with and without the propellers

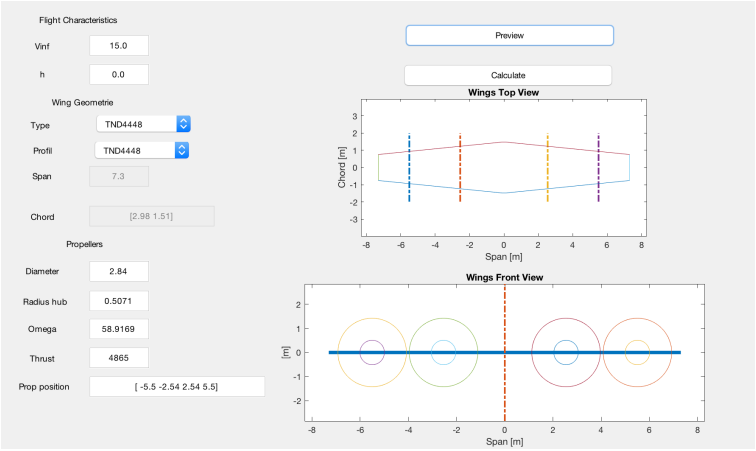

Figure 4: BLLT GUI representation for the propeller and wing parameters inputs

from wind-tunnel experiments. In the BVLM, the propellers are characterized one by one such that non-homogenoues thrust configurations are possible. This feature is important for future studies concerning the distributed propellers along the wing span. Figure 6 is the GUI representation of the required parameters for the propeller for BVLM.

Different test-cases have been simulated and compared with experimental data. The experimental data must be coherent with the condition of the practical use of this module : a large aspect ratio wing and a large Reynolds number. On a wing presenting small sweep and dihedral. For the verification with the TN D-4448 report purposes, the freestream velocity, V_∞ range from 15 to 25 m/s corresponding to the range of Re from 2.7 to 4.1 million. The input varied for the proposed BVLM, BLT and VSPAERO. The J and Tc' were extracted from Figure 4[19] for medium wing span, hence we get the C_T from equation 4 and equation 17. A few assumptions on the propeller efficiency are required to estimate the C_P values for each simulation since the information is not made available in the TN D-4448 report. The rotational speed and thrust of the propellers was also required for the computation. With the propellers involvement, the total thrust, T produced by the propellers dependence to the freestream velocity, V and wing surface area, S as follows

$$T = Tc' \frac{1}{2} \rho V^2 S \tag{17}$$

Another way of computing the thrust is with propeller characteristics as previously mentioned in equation 4 and 5. The non-dimensional advance ratio, J in equation 5 also represent the loading of the propeller blades. The advance ratio profile is inversely proportional to the loading of the propeller blades. Hence, the non-dimensional coefficients can also

DOI: 10.13009/EUCASS2017-445

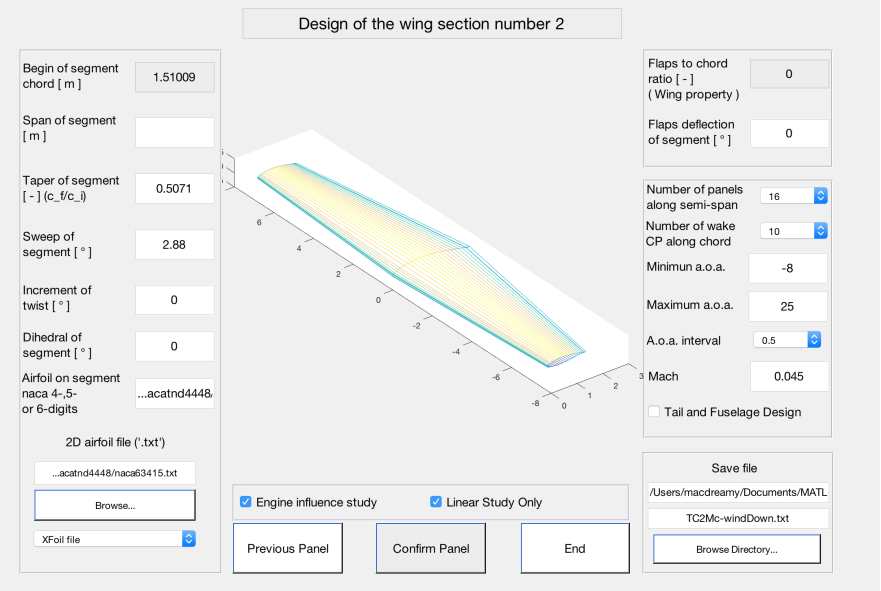

Figure 5: BVLM GUI representation for the wing parameters inputs

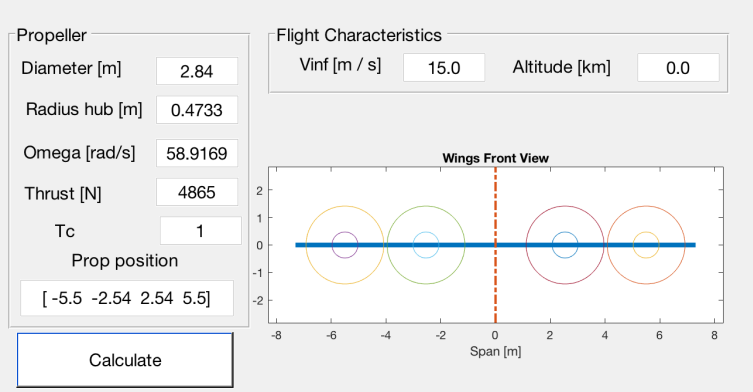

Figure 6: GUI representation of the propeller parameters input

defined the propeller efficiency as previously mentioned in equation 6.

4. Verification and Synthesis Results

Experimental measurements are extracted from the original report where the longitudinal characteristics of the model with and without the propeller operated comparisons were made to have a strong correlation for a considerably good initial conceptual design with the selected technical tools. Hence, the linearity approach projects significant accuracy in the area up to the airfoil section's stall angle.

4.1 Linear Decoupled Propeller-Wing Analysis

In this section, the propeller and wing aerodynamic models are decoupled. The first step taken is to review technical tools available as an attempt to mimic the NASA TN D-4448 test case. However, here, the performance of the propeller model alone is not presented. As only the wing model simulated, the expected time-averaged performance is kept to the minimum. Figure 7a shows the numerical measurements using three different VLM tools, namely, AVL, VSPAERO and BVLM. The behaviour of the models show excellent agreement for the lift coeffcient, C_L against angle of attack variations, α . Clearly, one of the significant points drawn from Figure 7a and 7b where both program is capable of predicting a much reliable results at lower angle of attack (-8 to 5 degree) as compared to higher angle of attack. The curvature does represents the linearity of the lifting surface method as what we desired and intercepted at zero-lift angle of attack, -2.5 degree. At higher angles, the discrepancies become more apparent by 25%. Figure 7b is focusing on the spanwise variation of the wing. On one hand, the maximum lift coefficient measured by the wind tunnel for short

DOI: 10.13009/EUCASS2017-445

wing span with an aspect ratio of 5.71 is slightly higher as compared to medium wing span. On the other, the computed numerical curve slope was found closer to the short wing span. These numerical computations performed is to have a basic longitudinal aerodynamic characteristics of the wing model before partially and fully immersed in the propeller slipstream.

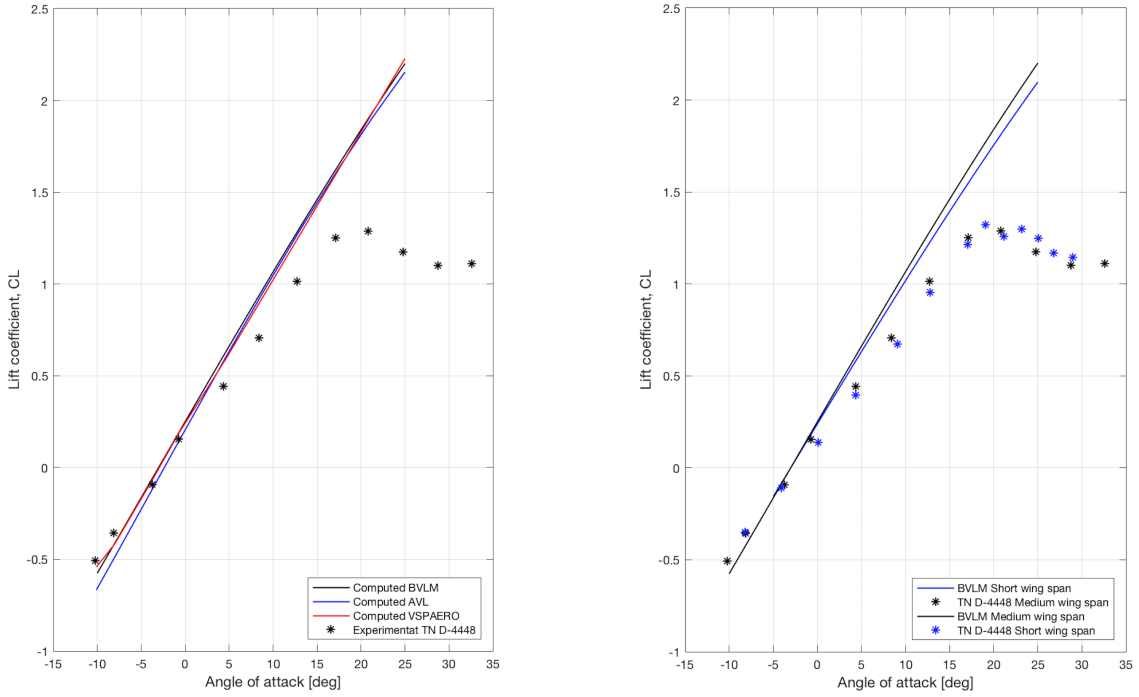

(a) Medium-span wing model with no propellers

(b) Medium and short-span wing with no propellers

Figure 7: Numerical and experimental measurement correlation based on $C_L - \alpha$ curve

4.2 Linear Propeller-wing Coupling Analysis

Current attention is being directed toward the effect of the propeller on the wing aerodynamic characteristics. The analysis carried out only considering the longitudinal flight dynamics, hence the lateral force and moments are assumed to be zero $F_y = M_x = M_z = 0$ as in equlibrium. Since the wing installation has no incidence angle, i_j the correction of the computed forces will only consider the angle of attack, α changes on the aircraft. The variation of α contribute to the changes of the longitudinal profile of the wing lift L_∞, drag D_∞, propeller thrust T,

$$F_z = L_\infty + \Sigma T \sin(\alpha + i_j) \tag{18}$$

$$F_x = D_\infty - \Sigma T \cos(\alpha + i_j) \tag{19}$$

$$\tag{20}$$

The effect of interaction on medium wing span performance illustrated in the lift polar plots of Figure 8 respectively shows several individual polars for different propeller advance ratios. Figure 8 clearly illustrates the lift augmentation through lift curves plotted for various advance ratios. As the propeller power increasing (decreasing J) the curves have shifted to the right and down. As we can see in Figures 8a, 8b, and 8c we can say that three different tools, specifically, VSPAERO, BLLT and BVLM presents a range of considerably satisfactory results for the conceptual and preliminary design step. The experimental data indicates that the lift curves have intercepted points at zero-lift angle of attack at -2.344 deg which were close to numerical approximations. It is clear that the propeller-wing combine method (BLLT and VSPAERO) tend to over-predicted the magnitude of the lift perturbations at higher angle of attack as a result of the slipstream effect from the propeller. Based on equation 13, the BLLT code have taken the total thrust to compute the induced velocity for each propeller which explain the higher discrepancies. Primarily, this version was limited to straight wings and linear studies, but the most recent versions (BVLM) show really good results for different wing

DOI: 10.13009/EUCASS2017-445

designs. Other points to highlight is the computational time and cost taken with BLLT is much less than VSPAERO where at the same time it provided considerably sufficient results.

On the contrary, the lift polar of BVLM prediction was slightly less than measured data which is also consistent with the drag polar. From the drag polar plotted in Figure 9 it appears that, the errors may come from the plotted data of the experimental values which is always slightly more than the given Tc' values. This explains the lower estimation plotted by the BVLM which is more coherent with the Tc' input values. Moreover, to better understand the lift generation with respect to the propeller rotation direction, propeller rotation directions were varied. Here, the orientation of the inboard propellers on each side of the wing induce wind down and the outboard propellers induce wind up on the inboard of the wing. With this orientation, separation began at low positive angles of attack and progressed rapidly to the leading edge of the wing. The direction of propeller rotation is such that the propellers on each side of the wing induce wind down on the inboard of the wing, the lift curve is slightly lower and stall lightly delyed on higher angle of attack. Those findings are almost insignificant. However, at higher Tc' when the engine induced velocity is clearly higher than the freestream velocity, the effects of the orientation of the rotational speed become more visible.

As for the findings projected on $C_L - \alpha$ curve illustrated in Figure 10 and 11 is to deduce the effect of the spanwise variation of propeller thrust across the wing span on the lift and drag characteristics of the model. A good agreement with the experimental data for both thrust coefficients are clearly visualized. Thus, it can be resumed that the short span wing is the most effective due to the wingtip visibility.

Apparently, with the code limitation of BLLT and VSPAERO lead to more robust code (BVLM) and it appears that plotted results on the lift and drag characteristics for three different thrust coefficients, $Tc' = 1.0$, 2.4 and 3.8 of the medium wing span, the BVLM designed code manage to compute the closest approximations. Additionally, the same trend plotted for the short wing span presented a very close correlation with the measured wind-tunnel data. The capability of the BVLM model to predict linear fit up to stall region was excellent due to the fact that it is coupled with the 2D viscous airfoil data. However, the tool is naturally highly dependant in the polar curves that are given by the user. It is highly recommended to provides polar curves that are really well adapted to the case that we want to study. It is important for the test that the airfoil polar data are coherent with the wing data. To be as much coherent as possible, the airfoil data that are used for the following cases come from the same wind-tunnel and the flow characteristics were kept identical as the experimental data for the wings. Furthermore, the tool has the capacity to consider a complete aircraft configuration i.e., the tail or other lifting surfaces and the fuselage effects.This ensures a gain in accuracy and keeps reasonable computational costs.

5. Conclusions and Perspectives

In this paper, the authors presented a rapid aerodynamic modelling to include the flow physics of propeller slipstream on the wing in the design process. As a results, the VSPAERO and BLLT have shown a considerably satisfactory computation with some discrepancies at higher angle of attack. Although the code have shown a lot of advantages for the propeller-wing interacton with a very minimum computational costs, some simplifications leads to a few limitations. Even though BLLT simulation is faster than VSPAERO, it is limited to wings with propellers, and does not concern fuselages, empennages or other part of the plane. A deeper understanding of the method, lead to a better lift and induced drag computation with BET coupled with VLM model. In this approach, the lifting surfaces such as aircraft wings, fins and canards modelled as an infinitely thin sheet of discrete vortices. The results of the low-cost model presented here is encouraging through good validation cases. It is also an indication that this approach promise a strong base for initial aerodynamic design simulations of wings with significant slipstream effects. Having said that, future enhancements forseen in expanding the tool for a non-linear analysis and take the compressibility and viscous effects into account. This extension allows the prediction of the stall region of the aerodynamic performances. As this project is part of multidisciplinary project that aimed at predicting the effects of a distributed propulsive systems along the span for regional aircraft, better prediction of the performance requires for the wing surface to be smaller with the extension to flapped wings configuration. Regardless, this work has open one of many doors of possible new design strategies to integrate the tool in the scope of the main MDO project for a rapid aero-propulsive analysis which indeed may reveal some performance benefits at the same time complement each other in increasing the fidelity level and lower the cost.

DOI: 10.13009/EUCASS2017-445

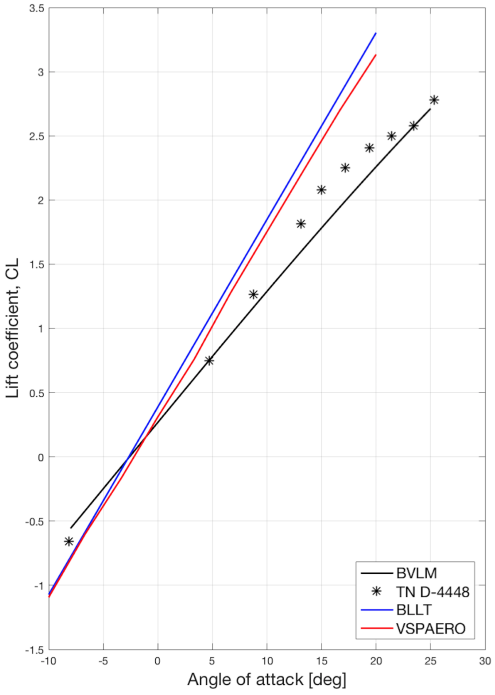

(a) Tc'=1.0

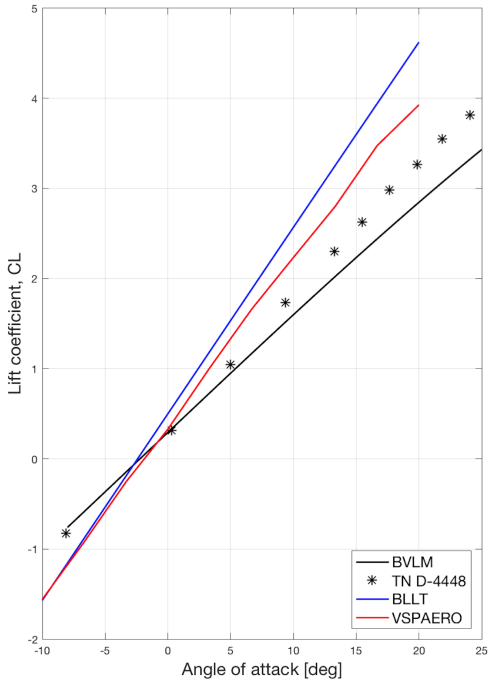

(b) Tc'=2.4

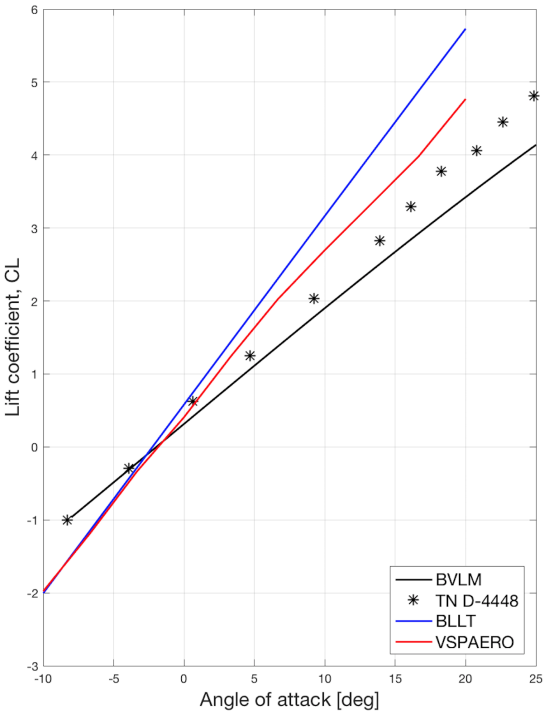

(c) Tc'=3.8

Figure 8: Comparison of the experimental and computational $C_L - \alpha$ curves for three different thrust coefficients

DOI: 10.13009/EUCASS2017-445

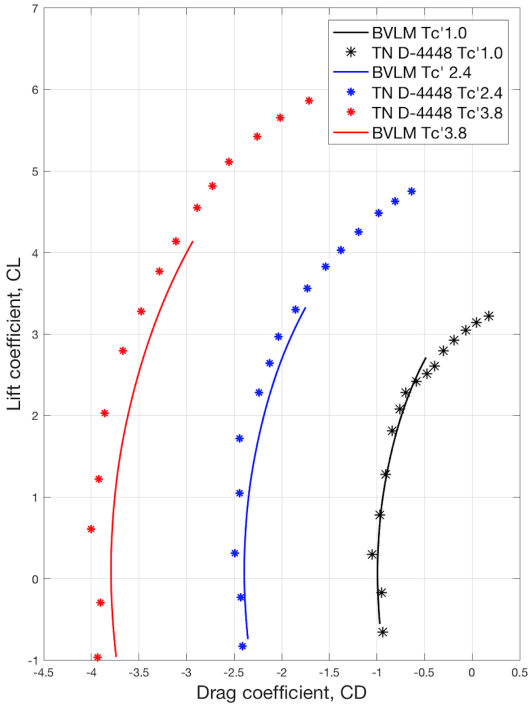

Figure 9: Comparison of the experimental and computational $C_L - C_D$ curves for medium wing span at three thrust coefficients

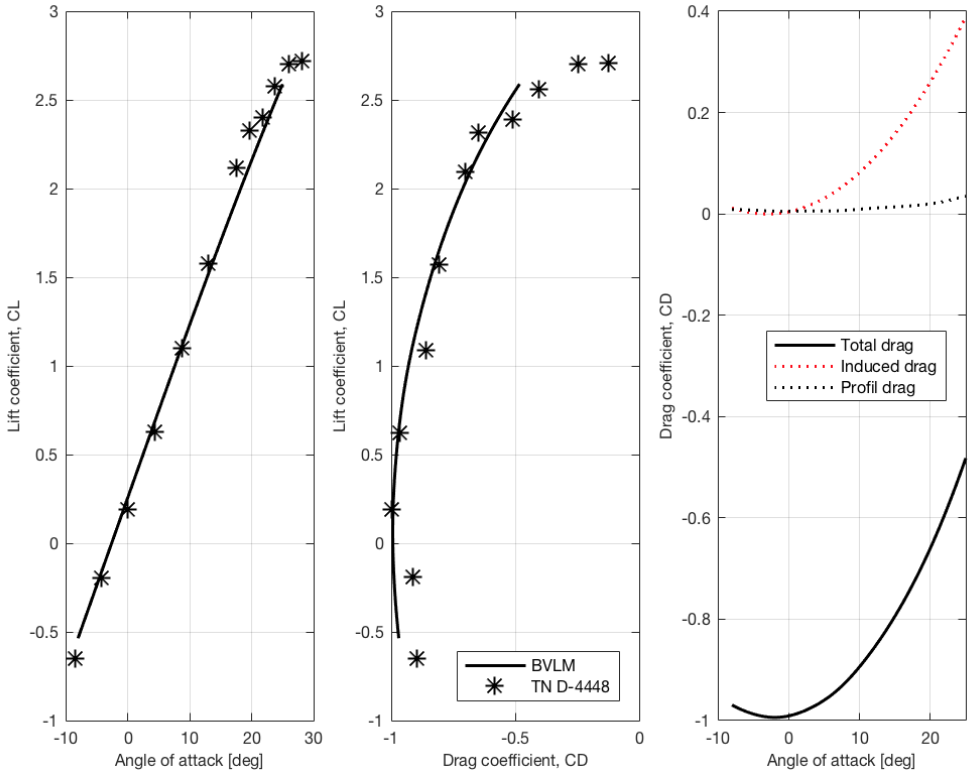

Figure 10: Comparison of the experimental and computational lift curves for short wing span at Tc'=1.0

6. Acknowledgments

The authors would like to thank Emmanuel Brandoli, former double degree student at ISAE-SUPAERO, for his important contribution in the development of the blade element and lifting line coupling aerodynamic prediction method.

DOI: 10.13009/EUCASS2017-445

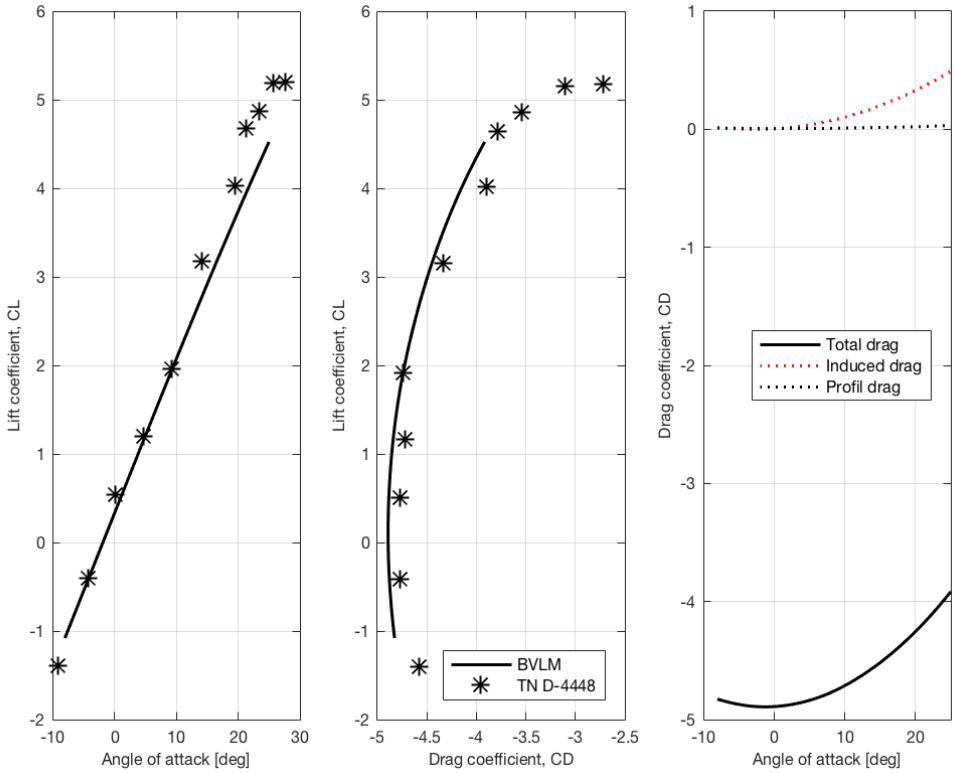

Figure 11: Comparison of the experimental and computational lift curves for short wing span at Tc'=4.9

References

[1] Christian Agostinelli, Simone Simeone, Abdul Rampurawala, Christian B Allen, and Feng Zhu. A Fast Approach to Model the Effects of Propeller Slipstream on Wing Load Distribution. In *53rd AIAA Aerospace Sciences Meeting*, AIAA SciTech, pages 1–12. American Institute of Aeronautics and Astronautics, jan 2015.

[2] Gregorio Ameyugo, Mark Taylor, and Riti Singh. Distributed Propulsion Feasibility Studies. *25th International Congress of the Aeronautical Sciences*, 2006.

[3] J. A. Blackwell. A finite-step method for calculation of theoretical load distributions for arbitrary lifting-surface arrangements at subsonic speeds. *NASA TN*, D-5335, 1969.

[4] Nicholas K. Borer, Joseph M. Derlaga, Karen A. Deere, Melissa B. Carter, Sally Viken, Michael D. Patterson, Brandon Litherland, and Alex Stoll. Comparison of Aero-Propulsive Performance Predictions for Distributed Propulsion Configurations. *55th AIAA Aerospace Sciences Meeting*, pages 1–16, 2017.

[5] Nicholas K. Borer and Mark D. Moore. Integrated Propeller - Wing Design Exploration for Distributed Propulsion Concepts. In *53rd AIAA Aerospace Sciences Meeting*, AIAA SciTech, pages 1–16. American Institute of Aeronautics and Astronautics, jan 2015.

[6] G. S. Campbell. A finite-step method for the calculation of span loadings of unusual plan forms. *NACA RM*, L50L13, 1951.

[7] Jean-Jacques Chattot. Actuator Disk Theory Steady and Unsteady Models. *Journal of Solar Energy Engineering*, 136(3):031012, 2014.

[8] Mark Drela. Mses. URL: http://web.mit.edu/drela/Public/web/mses/, December 4, 2015.

[9] Mark Drela and Harold Youngren. Xfoil. URL: http://web.mit.edu/drela/Public/web/xfoil/, Dec 23, 2013.

[10] Mark Drela and Harold Youngren. Avl 3.30 user primer. URL: http://web.mit.edu/drela/Public/web/avl/, Feb 12, 2017.

[11] Mark Drela and Harold Youngren. Xrotor. URL: http://web.mit.edu/drela/Public/web/xrotor/, Nov 13, 2013.

DOI: 10.13009/EUCASS2017-445

[12] Giovanna Ferraro, Timoleon Kipouros, Mark Savill, Abdul Rampurawala, and Christian Agostinelli. Propeller-Wing Interaction Prediction for Early Design. *AIAA SciTech 52nd Aerospace Science Meeting*, (January):1–13, 2014.

[13] Douglas Hunsaker and Deryl Snyder. A Lifting-Line Approach to Estimating Propeller / Wing Interactions. *AIAA Applied Aerodynamics Conference*, 26(3466), 2006.

[14] T. Jardin, G. Grondin, J. Gressier, C. Huo, N. Doué, and R. Barènes. Revisiting Froude's Theory for Hovering Shrouded Rotor. *AIAA Journal*, pages 1–9, 2015.

[15] Katz and Plotkin. *Low-Speed Aerodynamics*. Cambridge Aerospace Series, second edition edition, 2001.

[16] Andrew B. Lambe and Joaquim R. R. A. Martins. Extensions to the design structure matrix for the description of multidisciplinary design, analysis, and optimization processes. *Structural and Multidisciplinary Optimization*, 46(2):273–284, 2012.

[17] Rob McDonald. VSPAERO. URL: http://www.openvsp.org/, 2016.

[18] F Moens and P Gardarein. Numerical Simulation Of The Propeller / Wing Interactions For Transport Aircraft. *Transport*, (June), 2001.

[19] V. Robert Page, Stanley O. Dickinson, and Wallace H. Deckert. Large-scale wind-tunnel tests of a deflected slipstream STOL model with wings of various aspect ratios. Technical report, National Aeronautics and Space Administration, Washington, D. C., 1968.

[20] Michael D. Patterson, Joseph M. Derlaga, and Nicholas K. Borer. High-Lift Propeller System Configuration Selection for NASA's SCEPTOR Distributed Electric Propulsion Flight Demonstrator. In *16th AIAA Aviation Technology, Integration, and Operations Conference*, AIAA Aviation. American Institute of Aeronautics and Astronautics, jun 2016.

[21] Alex M Stoll. Comparison of CFD and Experimental Results of the LEAPTech Distributed Electric Propulsion Blown Wing. *15th AIAA Aviation Technology, Integration, and Operations Conference*, (June):22–26, 2015.

[22] Alex M. Stoll, Joeben Bevirt, Mark D. Moore, William J. Fredericks, and Nicholas K. Borer. Drag Reduction Through Distributed Electric Propulsion. *14th AIAA Aviation Technology, Integration, and Operations Conference*, (June):1–10, 2014.

[23] David Witkowski, Alex Lee, and John Sullivan. Aerodynamic interaction between propellers and wings. *26th Aerospace Sciences Meeting*, 26(9), 1988.